Preprints of the 18th IFAC World Congress
Milano (Italy) August 28 - September 2, 2011

Control of an underactuated manipulator using similarities to the double integrator

Carsten Knoll * **Klaus Röbenack** *

* *Institute of Control Theory, Faculty of Electrical and Computer Engineering, Technische Universität Dresden, 01062 Dresden, Germany (Tel: +49351-463-33268; e-mail: {Carsten.Knoll, Klaus.Roebenack}@tu-dresden.de).*

Abstract: A horizontally mounted two-link manipulator is considered. We assume that only the first joint is actuated, while the second joint is passive and frictionless. The system exposes challenging properties, e. g. it is not controllable in the equilibrium points. We transform the equations of motion in Byrnes-Isidori normal form and consider the projection into the subspace spanned by the velocity-like state variables. From this viewpoint the manipulator system reveals qualitative similarities to the well-understood double integrator. In particular the drift vector field is investigated. Exploiting these similarities, an approach for equilibrium point transition based on sliding mode control is proposed.

Keywords: underactuated manipulator, double integrator, Byrnes-Isidori normal form, sliding mode, point symmetry

1. INTRODUCTION

The control of mechanical systems has been one of the main fields of interest of control theory since its beginnings. Especially interesting are so-called *underactuated* systems with fewer actuators (control inputs) than degrees of freedom (see, e. g. Bullo and Lewis (2004)).

Many mechanical control systems are underactuated "by nature", e. g. several types of vehicles which are considered in Wichlund et al. (1995). In other cases, the interest in underactuated systems arises from efforts of saving costs or weight by using fewer actuators than usually. Being able to control an originally fully actuated system in the case of actuator failure is another motivation for investigating such systems.

In this contribution we consider the two-link manipulator depicted in Fig. 1. We assume that the manipulator is mounted horizontally such that the gravity has no influence on the system. The joint connecting the first link with the inertial system is actuated, i. e., the applied torque is the system's input. The second joint is passive and assumed to be frictionless, which means that no torque acts on it. Obviously, this system is underactuated.

Some underactuated systems can be addressed by means of linear control theory, e. g. the famous pole-cart system. Unfortunately, the linearization of the manipulator system is not controllable in any equilibrium point. Moreover, there is no continuous state feedback which stabilizes a given equilibrium point since the Brockett condition is violated, (see Brockett (1983); Oriolo and Nakamura (1991)). In addition, Oriolo and Nakamura (1991) give a PD control law which stabilizes the first joint at a given position while the rest point of the second joint depends on the initial conditions.

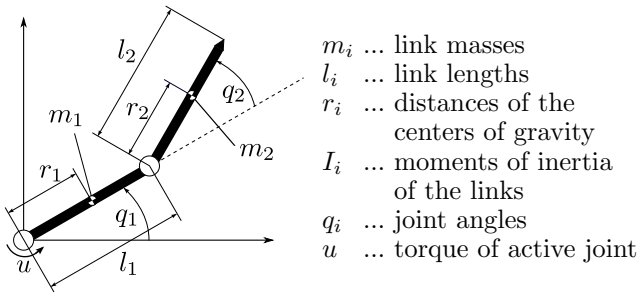

Figure 1. Underactuated two link manipulator in horizontal plane (top view).

Because of these challenging properties many researchers investigated this system since the beginning of the 1990s. The main interest lies in point to point control. In Arai and Tachi (1991) and Mareczek et al. (1999), the problem is simplified by assuming a holding brake in the passive joint [1]. This allows to decouple the motions of the two joints, i. e., the passive joint reaches its final position first, and the active joint is positioned thereafter. In Mahindrakar et al. (2006), a significant Coulomb friction is assumed and explicitly utilized for motion planning. Under certain constraints, this type of friction has a similar effect as a holding brake. In Scherm and Heimann (2001), the system dynamics is considered as time discrete and a feasible input trajectory is obtained by a numerical optimization routine. Alternatively, this could be seen as a shooting method for solving the corresponding boundary value problem. As above, the underlying model has a significant Coulomb friction which causes the resulting motion to be decoupled as well.

[1] The holding brake used in the cited contributions is not classified as an actuator in the sense of a continuous control input. To apply the brake means that the system is subject to an additional holonomic constraint, which changes the degrees of freedom and therefore the system's structure.

Another category of approaches is based on a model without friction and holding brake. For example, Suzuki et al. (1996) suggest a suitable modulation of the amplitude of a periodic input signal in order to achieve point-to-point transition. A second example of this group is proposed in De Luca et al. (1997). This approach relies on a so-called nilpotent approximation of the system, which allows the construction of a set of maneuvers iteratively performing the desired transition. Both approaches result in rather complex motions and require high actuator activity.

Of course, many other challenging underactuated systems are investigated in the literature, see Bullo and Lewis (2004) and the references cited there. In some cases, sliding mode control has successfully been applied, cf. Ashrafiuon and Erwin (2008) and Riachy et al. (2008).

The paper is organized as follows. In Section 2 the equations of motion are derived and partial linearization is performed. Finally, the system equations are transformed into Byrnes-Isidori normal form. Based on this representation we point out the relation between the manipulator dynamics and the double integrator in Section 3. This relation is used in Section 4 to construct a controller scheme which under certain conditions reaches some equilibrium point. An approach to extend this controller to perform a complete point-to-point control is sketched in Section 5.

2. MANIPULATOR MODEL

The manipulator model shown in Fig. 1 can be interpreted as a double pendulum lacking potential forces. Its kinetic energy reads as

$$T = \frac{1}{2}(a_1\dot{q}_1^2 + a_2(\dot{q}_1+\dot{q}_2)^2 + 2a_3\dot{q}_1(\dot{q}_1+\dot{q}_2)\cos q_2) \quad (1)$$

with the parameters $a_1 = I_1+m_1r_1^2+m_2l_1^2$, $a_2 = I_2+m_2r_2^2$ and $a_3 = m_2l_1r_2$. From (1) the equations of motion can be derived:

$$\mathbf{M}(\mathbf{q})\ddot{\mathbf{q}} + \mathbf{C}(\mathbf{q},\dot{\mathbf{q}}) = (u,0)^T \ . \quad (2)$$

In this equation we have the vectors of angles $\mathbf{q} = (q_1,q_2)^T$, angular velocities $\dot{\mathbf{q}}$, and angular accelerations $\ddot{\mathbf{q}}$. The mass matrix $\mathbf{M} = (M_{ij})$ has the form

$$\mathbf{M}(\mathbf{q}) = \begin{pmatrix} a_1+a_2+2a_3\cos q_2 & a_2+a_3\cos q_2 \\ a_2+a_3\cos q_2 & a_2 \end{pmatrix} \ , \quad (3)$$

and

$$\mathbf{C}(\mathbf{q},\dot{\mathbf{q}}) = \begin{pmatrix} C_1 \\ C_2 \end{pmatrix} = a_3\sin q_2 \begin{pmatrix} -(2\dot{q}_1\dot{q}_2+\dot{q}_2^2) \\ \dot{q}_1^2 \end{pmatrix} \quad (4)$$

is the vector of the centrifugal and Coriolis forces. The input u denotes the torque of the actuated joint. We assume that both joints do not possess limitations. As we have two rotational degrees of freedom, we can identify the points given by $q_i + 2\pi$ with those given by q_i, where $i = 1,2$. In other words, the configuration manifold is the torus $\mathbb{S}^1 \times \mathbb{S}^1$. In order to keep the notation simple, we do, however, not introduce multiple coordinate charts but instead consider $0 \le q_i < 2\pi$, with $i = 1,2$.

The system equations (2)-(4) can be simplified considerably if input-output linearization is performed (Isidori (1995)). To do this, (2) must be solved for the angular accelerations. Then, one has to choose one of the coordinates as output and define a feedback law which introduces a new input, v, which corresponds to the second time derivative of the chosen coordinate. As stated in Spong (1998) partial linearization always is possible for collocated outputs, i. e., coordinates corresponding to the actuated joints. More precisely, the resulting feedback law contains no singularity.

Hence, the coordinate x_1 is chosen as output which leads to the feedback law

$$u = C_1 + \frac{\det\mathbf{M}}{M_{22}}\left(v - \frac{M_{12}}{\det\mathbf{M}}C_2\right). \quad (5)$$

Furthermore, the state vector

$$\mathbf{x} = (x_1,x_2,x_3,x_4)^T = (q_1,\dot{q}_1,q_2,\dot{q}_2)^T \quad (6)$$

is introduced. Now, the system dynamics simplifies to

$$\dot{\mathbf{x}} = \begin{pmatrix} x_2 \\ 0 \\ x_4 \\ -\eta\sin x_3 x_2^2 \end{pmatrix} + \begin{pmatrix} 0 \\ 1 \\ 0 \\ -(1+\eta\cos x_3) \end{pmatrix} v \ , \quad (7)$$

where the only remaining parameter is the dimensionless ratio

$$\eta := \frac{a_3}{a_2} = \frac{m_2l_1r_2}{I_2+m_2r_2^2} \ . \quad (8)$$

Further on we assume[2] $0 < \eta < 1$, which is known as *strong inertial coupling* (Spong (1998)). An useful observation pertains the case of vanishing x_2 and v. This implies that $\dot{x}_4 = 0$, which means that the second arm circulates at constant angular velocity. Due to the rotational nature of the second joint (i.e., $q_2 \in \mathbb{S}^1$), every possible configuration of that joint can be reached simply by waiting.

In (7) the input v appears in the linear subsystem (second line) as well as in the nonlinear one (fourth line). Using the state transformation

$$z_i = x_i \ , \quad \text{for } i = 1,2,3 \quad (9a)$$
$$z_4 = x_4 + (1+\eta\cos x_3)x_2 \ , \quad (9b)$$

which is a global diffeomorphism, the appearance of the input in the nonlinear subsystem can be eliminated:

$$\begin{aligned}\dot{z}_4 &= \tfrac{\mathrm{d}}{\mathrm{d}t}\left[x_4 + (1+\eta\cos x_3)x_2\right] \\ &\overset{(7),(9)}{=} \eta z_2\sin z_3(\eta z_2\cos z_3 - z_4) =: f_4(\mathbf{z}) \ . \end{aligned} \quad (10)$$

The change of coordinates (9) transforms system (7) into Byrnes-Isidori normal form:

$$\begin{pmatrix} \dot{z}_1 \\ \dot{z}_2 \\ \dot{z}_3 \\ \dot{z}_4 \end{pmatrix} = \underbrace{\begin{pmatrix} z_2 \\ 0 \\ z_4 - (1+\eta\cos z_3)z_2 \\ f_4(\mathbf{z}) \end{pmatrix}}_{=:\mathbf{f}(\mathbf{z})} + \underbrace{\begin{pmatrix} 0 \\ 1 \\ 0 \\ 0 \end{pmatrix}}_{=:\mathbf{g}(\mathbf{z})} v \ . \quad (11)$$

From (9) we obtain

$$x_2 = x_4 = 0 \Leftrightarrow z_2 = z_4 = 0 \ , \quad (12)$$

which means that all equilibrium points are located in the origin of the z_2-z_4-plane.

Remark: It is straightforward to show that a construction similar to (9b) can always be used to obtain the normal

[2] The condition $0 < \eta$ implies $r_2 > 0$. Otherwise, i.e., if $\eta = 0$, the system degenerates to two decoupled double integrators. The condition $\eta < 1$ ensures that M_{21} is positive for all configurations. Hence, a non-collocated input output linearization would be possible, too. However, that would lead to a zero dynamics with finite escape time and is therefore not considered here.

form from an input-output linearized form of an underactuated system. This is due to the fact that the new input affects the nonlinear subsystem through a (vector-valued) function which does not depend on the velocities.

3. ANALOGIES TO THE DOUBLE INTEGRATOR

The main challenge of the equilibrium point transition consists in reaching an equilibrium point at all. This requires to control both angular velocities to zero *at the same time*, using the single input. Considering the normal form representation of the underactuated manipulator, this control task corresponds to reaching the origin of the z_2-z_4-plane. Projecting the system dynamics into this subspace of the state space,

$$\frac{d}{dt}\begin{pmatrix} z_2 \\ z_4 \end{pmatrix} = \underbrace{\begin{pmatrix} 0 \\ f_4(\mathbf{z}) \end{pmatrix}}_{=:\,\bar{\mathbf{f}}(\mathbf{z})} + \underbrace{\begin{pmatrix} 1 \\ 0 \end{pmatrix}}_{=:\,\bar{\mathbf{g}}} v \ , \tag{13}$$

reveals a remarkable similarity to a double integrator. We augment the standard double integrator allowing a possible change of sign between the two integrators. The (modified) double integrator can be described by the state-space system:

$$\frac{d}{dt}\begin{pmatrix} \tilde{y} \\ \tilde{x} \end{pmatrix} = \underbrace{\begin{pmatrix} 0 \\ \sigma\tilde{y} \end{pmatrix}}_{=:\,\tilde{\mathbf{f}}_\sigma} + \underbrace{\begin{pmatrix} 1 \\ 0 \end{pmatrix}}_{=:\,\tilde{\mathbf{g}}} \tilde{v} \ \text{ with } \ \sigma \in \{-1, +1\} \ . \tag{14}$$

The structural similarity between (13) and (14) immediately becomes apparent. Clearly, the input vector fields are equal. In both cases the two vector fields are parallel to the axes in the Cartesian plane. In particular, the drift vector field is parallel to the vertical axis and orthogonal to the input vector field. Of course the drift term of the manipulator is more complex than the drift term of the double integrator. But, as we will see, there are subsets of the state space where they match at least qualitatively (in the sense of topological equivalence) whether the drift points towards the abscissa axis or away from it.

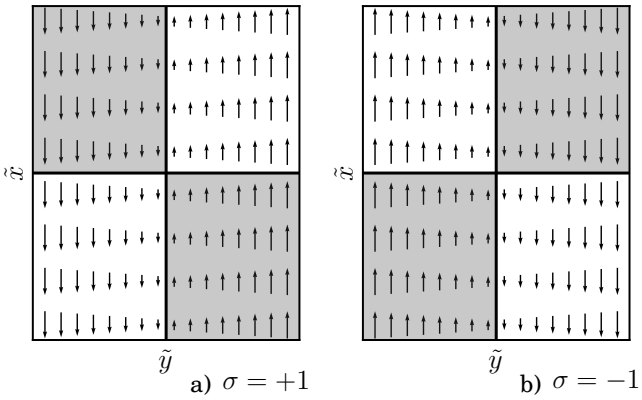

Figure 2. Drift vector field of the (modified) double integrator.

Fig. 2 shows the drift vector field of the double integrator (14). In case of $\sigma = +1$, the drift causes the trajectories starting in the second and fourth quadrant to approach the horizontal axis while in the remaining two quadrants the system moves away from it, see Fig. 2(a). In case of $\sigma = -1$, the trajectories starting in the first and third quadrant approach the horizontal axis as shown in Fig. 2(b). On the vertical axis, where $\tilde{y} = 0$, the drift vanishes.

For the projected manipulator dynamics (13) the situation is different, but not completely different. Sign and magnitude of the drift are determined by z_2, z_3 and z_4. From (10) it is obvious that on the (vertical) z_4 axis the drift term is zero as well. However, there is another straight line in the z_2-z_4-plane, given by

$$z_4 = (\eta \cos z_3)\, z_2 \ , \tag{15}$$

on which the drift vanishes. Its slope varies with z_3 and takes values between $\pm\eta$. On each side of both lines the drift term takes a different sign. Together with the factor $\sin z_3$, this varying slope implies that there are four qualitatively distinct drift situations in the z_2-z_4-plane. Each of them corresponds to one of the four intervals given by

$$\mathcal{I}_i := \left(\tfrac{i-1}{2}\pi, \tfrac{i}{2}\pi\right) \quad \text{with } i = 1, ..., 4 \ . \tag{16}$$

Fig. 3 illustrates this situation.

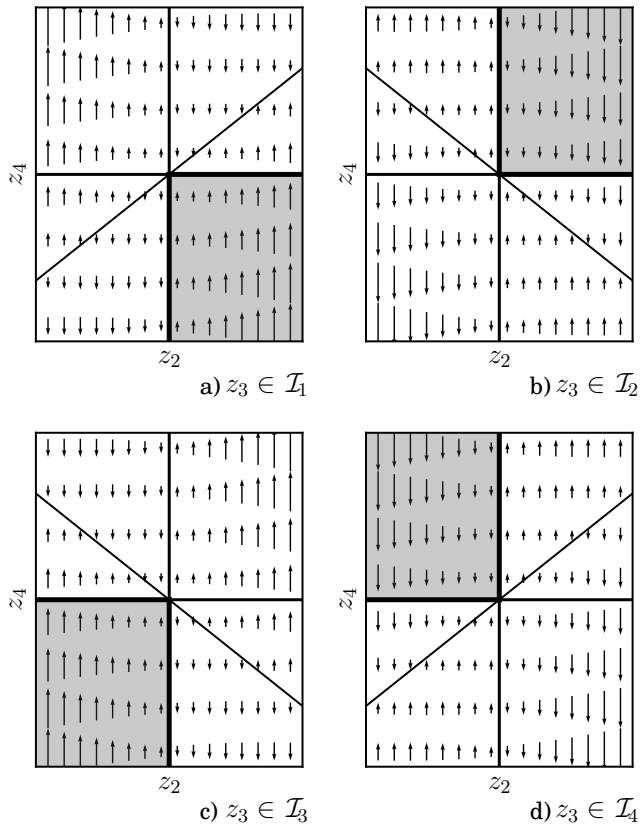

Figure 3. Drift vector field of the projected manipulator dynamics (13). Each picture shows one of the four relevant cases. The diagonal line indicates where the drift changes its sign, see Eq. (15).

One can see that for every $z_3 \neq k\frac{\pi}{2}$, $k = 0, ..., 3$ there is always one complete quadrant in which the drift brings the system closer to the origin. This region will be of importance for the controller scheme developed in Section 4. At the isolated z_3 values where this condition is not fulfilled,

either the drift vanishes everywhere in the plane due to $\sin z_3 = 0$, or the the straight line with varying slope coincides with the z_2 axis due to $\cos z_3 = 0$. In both cases, a transition from one of the four cases of Fig. 3 to another takes place. Therefore $k\frac{\pi}{2}$ are critical values for z_3, which should be avoided.

From Eq. (11) we deduce that $z_2 = 0$ implies $z_4 \equiv \dot{z}_3$. As stated above, the drift vanishes for $z_2 = 0$, i.e., the system does not move in the z_2-z_4-plane. In this "parking regime" of (13), the second arm of the manipulator circulates with constant velocity as described in the previous section. This property will play an important role for the equilibrium point transition discussed in Section 5. Note that for a given value of $|\dot{z}_3|$ there are two parking regimes which differ only in the sign of z_4.

Summarizing, it can be stated that the z_2-z_4-dynamics (13) of the manipulator system (for almost all z_3 values) has one quadrant in which the drift conditions qualitatively match that of the modified double integrator (14). Furthermore, assuming $z_2 = 0$ and $z_4 \neq 0$, every possible drift situation can be achieved by waiting. Basing on these two properties we can adapt an existing control approach for the double integrator, in order to reach the origin of the z_2-z_4-plane i. e., to steer the underactuated manipulator into an equilibrium point.

4. REACHING AN EQUILIBRIUM POINT

In this section we design a controller which performs a "braking maneuver", i. e., which drives the underactuated manipulator into an equilibrium point in finite time. To do this, we exploit the structural similarities to the double integrator so we can adapt the sliding mode controller proposed in Bhat and Bernstein (1998) to stabilize that system at the origin, cf. also Knoll and Röbenack (2010).

We define the sliding surface by a curve in the z_2-z_4-plane:

$$z_2 = \varphi(z_4). \tag{17}$$

Proposition 1. The feedback law

$$v = \varphi'(z_4) f_4(\mathbf{z}) - \gamma_1 \operatorname{sign}(\Phi(\mathbf{z}))|\Phi(\mathbf{z})|^{\gamma_2} \tag{18}$$

with $\gamma_1 > 0$ and $\gamma_2 \in (0, 1)$ renders the sliding surface given by

$$\Phi(\mathbf{z}) := z_2 - \varphi(z_4) = 0 \tag{19}$$

as an attractive and invariant set.

Proof. Following Slotine and Li (1991), Chapter 7, we have

$$\begin{aligned} \tfrac{1}{2}\tfrac{d}{dt}\Phi^2(\mathbf{z}) &= \Phi(\mathbf{z})\,\dot{\Phi}(\mathbf{z}) \\ &= \Phi(\mathbf{z})\,(\dot{z}_2 - \varphi'(z_4)\,\dot{z}_4) \\ &= \Phi(\mathbf{z})\,(v - \varphi'(z_4) f_4(\mathbf{z})) \\ &= -\gamma_1 |\Phi(\mathbf{z})|^{1+\gamma_2} \leq 0 \ , \end{aligned} \tag{20}$$

which shows attractiveness and invariance of (19). □

Remark: While the first term of the right hand side of (18) accounts for the nominal dynamics along the sliding surface, the second term serves to stabilize the system to the surface.

For reaching the origin, the curve defined by (17) must lie in the "double-integrator-like" quadrant of the plane. Furthermore, it must be tangent to the z_2-axis at $z_2 = 0$ because the drift vanishes for $z_2 \to 0$.

We assume $z_3 \in \mathcal{I}_2$ and consider the first quadrant Σ_1 as a subset of the state space:

$$\Sigma_1 := \{\mathbf{z} \in [0, 2\pi) \times \mathbb{R} \times (\tfrac{1}{2}\pi, \pi) \times \mathbb{R} \,|\, z_2, z_4 > 0\} \ . \tag{21}$$

Then the two requirements are fulfilled if the power function

$$\varphi(z_4) := (\mu\beta|z_4|)^{\frac{1}{\beta}} \tag{22}$$

with $\mu > 0$ and $2 < \beta < 3$ is used.

Proposition 2. As long as $\mathbf{z} \in \Sigma_1$ and $\Phi(\mathbf{z}) = 0$ hold, the feedback law (18) with (22) guarantees that the system reaches an equilibrium point in finite time.

Proof. On the sliding surface (19) we have

$$z_4 = \varphi^{-1}(z_2) = \tfrac{1}{\mu\beta} z_2^{\beta} \quad \text{and} \quad \varphi'(\varphi^{-1}(z_2)) = \mu z_2^{1-\beta} \ .$$

This can be substituted into (18), which leads to

$$\begin{aligned} \dot{z}_2 = v &= \varphi'(z_4)\dot{z}_4 \\ &= \varphi'(\varphi^{-1}(z_2)) f_4((\mathbf{z})) \\ &= \mu\eta^2 z_2^{3-\beta} \sin(2z_3) - \tfrac{\eta}{\beta} z_2^2 \sin z_3 \ . \end{aligned} \tag{23}$$

Because of $z_3 \in (\frac{\pi}{2}, \pi)$, which results from $\mathbf{z} \in \Sigma_1$, both terms of the sum are negative. To estimate an upper bound, the second term can thus be neglected. Additionally, we can always find a $k > 0$, such that the following inequality holds:

$$\dot{z}_2 < -\mu\eta^2 k z_2^{3-\beta} < 0. \tag{24}$$

We now consider the simple initial value problem

$$\dot{x} = -\tilde{k} x^{3-\beta} \ \text{ with } \ \tilde{k}, \beta > 0, \ \ t \geq 0 \ \text{ and } \ x(0) > 0 \tag{25}$$

for comparison. Using the separation method we obtain the solution

$$x(t) = (x(0)^{\beta-2} - (\beta - 2)\tilde{k}\, t)^{\frac{1}{\beta-2}}. \tag{26}$$

From this expression one can see, that $x(t) = 0$ is reached after finite time. Under the given assumptions, the right hand side of (23) is always smaller than the right hand side of (25). Therefore, z_2 goes to zero after finite time as well. □

The extension of this result to $\mathcal{I}_1, \mathcal{I}_3, \mathcal{I}_4$ and the corresponding quadrants is straightforward. However, the assumption $\mathbf{z} \in \Sigma_1$ is not guaranteed to hold during the deceleration maneuver. To be precise, $z_3 > \frac{1}{2}\pi$ is the crucial part of the condition. We can deduce from (11) that $\dot{z}_3 < 0$ holds in a large subset of Σ_1. That means, that during the (intended) braking maneuver z_3 could fall below $\frac{\pi}{2}$ and thus the drift term $f_4(\mathbf{z})$ would change its sign. This, however, would make it impossible to reach the origin.

As a consequence, the initial conditions of the braking maneuver must be restricted further, to a subset of Σ_1. The bounds of that subset can not be given explicitly, but an approximation can be calculated by numerical integration in backward time. Fig. (4) illustrates that subset in the z_3-z_4-plane. The black curve corresponds to the corner case where the equilibrium is reached with (nearly) $z_3 = \frac{\pi}{2}$.

Fig. 5 shows the projection of a trajectory of the manipulator system subject to the feedback (18) together with (22). The first part of the motion consists in reaching the sliding surface. Once in sliding regime, the origin is reached. We used the initial conditions $z_2(0) = 1\mathrm{s}^{-1}$, $z_3(0) = \frac{3}{4}\pi$ and $z_4(0) = 0.3\mathrm{s}^{-1}$. Because z_1 is a cyclic variable its value is not of interest here.

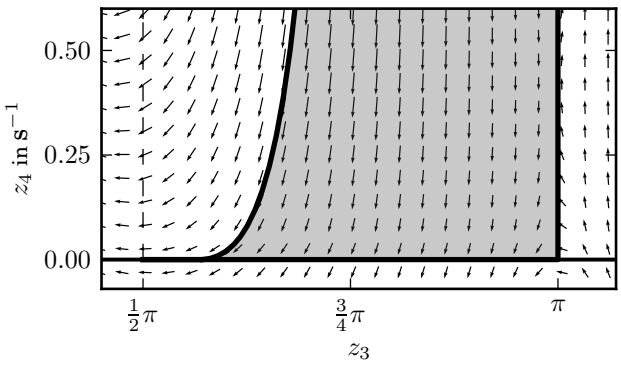

Figure 4. Vector field of the reduced dynamics projected to the z_3-z_4 plane. Arrow lengths adapted for better perceptibility. The domain of attraction is highlighted.

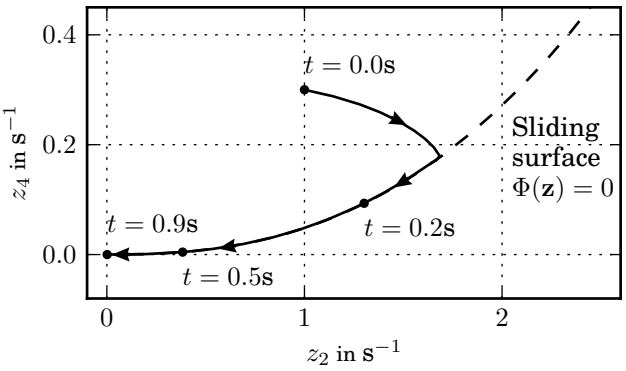

Figure 5. Simulation result demonstrating how an equilibrium point is reached (projection to the z_2-z_4-plane).

5. EQUILIBRIUM POINT TRANSITION

In the previous section it was shown that it is possible to reach *some* equilibrium point. However, the typical control objective is the transition from one equilibrium point to another. In other words, it is necessary to halt at a *given* configuration. To achieve this, we split up the whole transition process into four maneuvers (A-D) which are performed sequentially. For each of them a sliding mode controller similar to the one described above can be used. Between the maneuvers the system remains in the parking regime. Thus, the required drift conditions can be achieved simply by waiting.

5.1 Final Breaking Maneuver

The right hand side of (11) does not depend on z_1. Hence, we ignore the angle of the first joint for now and concentrate on reaching a given value z_3, say z_3^{d}. The easiest way to do this, is to vary the initial conditions of the braking maneuver (D). We assume that $z_3^{\mathrm{d}} \in \mathcal{I}_2$. It follows from Fig. 3 that the sliding surface has to lie in the first quadrant of the z_2-z_4-plane. Additionally we assume that the system is in the appropriate parking regime, i. e., $z_2 = 0$ and z_4 is a positive constant, say z_4^{p}.

The sliding surface for the breaking maneuver should therefore contain the points $(0, z_4^{\mathrm{p}})$ and $(0, 0)$. Furthermore the tangent in both points has to be parallel to the z_2-axis. Extending the approach (22) we define

$$\varphi(z_4) := \begin{cases} (\mu\beta|z_4|)^{\frac{1}{\beta}} \ , & \text{if } \frac{z_4^{\mathrm{p}} - z_4}{z_4^{\mathrm{p}}} > \frac{1}{2} \\ (\mu\beta|z_4^{\mathrm{p}} - z_4|)^{\frac{1}{\beta}} \ , & \text{else,} \end{cases} \tag{27}$$

which fulfills these conditions. Due to the properties of the parking regime, every possible initial condition for z_3 can be achieved by waiting. For a given z_3^{d} the necessary start value of z_3 can be determined by numerically solving the system dynamics during the sliding mode in backward time. This procedure yields as well the displacement Δz_1 of the first joint which is caused by the braking maneuver. Because (11) is independent of z_1, the the necessary initial value z_1^* can simply be determined by

$$z_1^* = z_1^{\mathrm{d}} - \Delta z_1, \tag{28}$$

where z_1^{d} denotes the desired final value of the first joint.

This approach for reaching equilibrium points with $z_3^d \in \mathcal{I}_2$ through the first quadrant of the z_2-z_4-plane can straightforwardly be adapted to reach equilibrium points with $z_3^d \in \mathcal{I}_3$. To cover the remaining two cases $z_3^d \in \mathcal{I}_1$ and $z_3^d \in \mathcal{I}_4$, the same principle can be used but the shape of the sliding surface must be modified.

Due to the vanishing drift near the z_2-axis for $z_3 = k\frac{\pi}{2}$, with $k = 0, ..., 3$, the duration of the maneuvers increases strongly for z_3-values near the boundaries of the intervals. Therefore, we define the admissible intervals

$$\tilde{\mathcal{I}}_i := \left(\tfrac{i-1}{2}\pi + \varepsilon, \tfrac{i}{2}\pi - \varepsilon\right) \quad \text{with } i = 1, ..., 4, \tag{29}$$

where ε is a small positive constant. In simulation studies good results were obtained e. g. for $\varepsilon = \frac{\pi}{15}$.

5.2 Symmetry Properties

Solving the system dynamics in backward time corresponds to solving it in forward time with suitable adapted initial conditions. If the manipulator system is in sliding regime the system dynamics is described by

$$\dot{z}_3 = z_4 - (1 + \eta\cos z_3)\varphi(z_4) =: \bar{f}_3(z_3, z_4) \tag{30a}$$

$$\dot{z}_4 = \eta\varphi(z_4)\sin z_3(\eta\varphi(z_4)\cos z_3 - z_4) =: \bar{f}_4(z_3, z_4)\ . \tag{30b}$$

Evidently, the point symmetry

$$\bar{f}_3(-z_3, z_4) = \ \ \bar{f}_3(z_3, z_4) \tag{31a}$$

$$\bar{f}_4(-z_3, z_4) = -\bar{f}_4(z_3, z_4) \tag{31b}$$

holds, which enables us to construct new solutions from existing solutions: Let $z_3(t), z_4(t)$ be a solution of (30) for $t \in [0, \tau]$, then another solution for the same interval is obtained by

$$\tilde{z}_3(t) := -z_3(\tau - t) \tag{32a}$$

$$\tilde{z}_4(t) := \ \ z_4(\tau - t)\ . \tag{32b}$$

This property follows immediately from a short consideration. We build the time derivative of $\tilde{z}_3$ and $\tilde{z}_4$, apply the symmetry (31) and then substitute using (32),

$$\dot{\tilde{z}}_3(t) = \bar{f}_3(\underbrace{-z_3(\tau - t)}_{\tilde{z}_3(t)}, \underbrace{z_4(\tau - t)}_{\tilde{z}_4(t)}) \tag{33a}$$

$$\dot{\tilde{z}}_4(t) = \bar{f}_4(\underbrace{-z_3(\tau - t)}_{\tilde{z}_3(t)}, \underbrace{z_4(\tau - t)}_{\tilde{z}_4(t)})\ , \tag{33b}$$

to obtain the system dynamics of (30).

A useful implication of property (32) is, that sliding surfaces which serve for transition into an equilibrium point (maneuver D) as well can be used to drive the

system from rest to parking regime, i. e., to perform the acceleration maneuver (A).

5.3 Further Maneuvers

Providing the right initial conditions for z_1 is the objective of a preceding maneuver (C). This can also be performed by stabilizing the system dynamics to a suitable sliding surface. In particular, a sliding surface is chosen, such that the motion starts and ends in the parking regime. The amount of the displacement of z_1 can be influenced by changing the shape of the curve φ.

So far, a desired equilibrium point can be reached if the system is in the appropriate parking regime.

As can be deduced from Fig. 3, depending on the value of z_3 in the initial equilibrium, the drift conditions permit to reach one of the two possible parking regimes with the acceleration maneuver. Of course, it can occur that maneuver A reaches just that parking regime with $z_4^{\mathrm{p}} > 0$ while maneuver D has to start in the one where $z_4^{\mathrm{p}} < 0$ or vice versa. Then, a maneuver is needed which transfers the system between the two parking regimes (B). Because the drift term $f_4(\mathbf{z})$ necessarily changes its sign this maneuver can not be performed completely on a sliding surface. Instead, the initial part can be done e. g. by choosing $v = \text{const}$, such that, the system roughly moves in the right direction. After the sign change of $f_4(\mathbf{z})$ has occurred, the system can be stabilized to a sliding surface on which it reaches the desired parking regime.

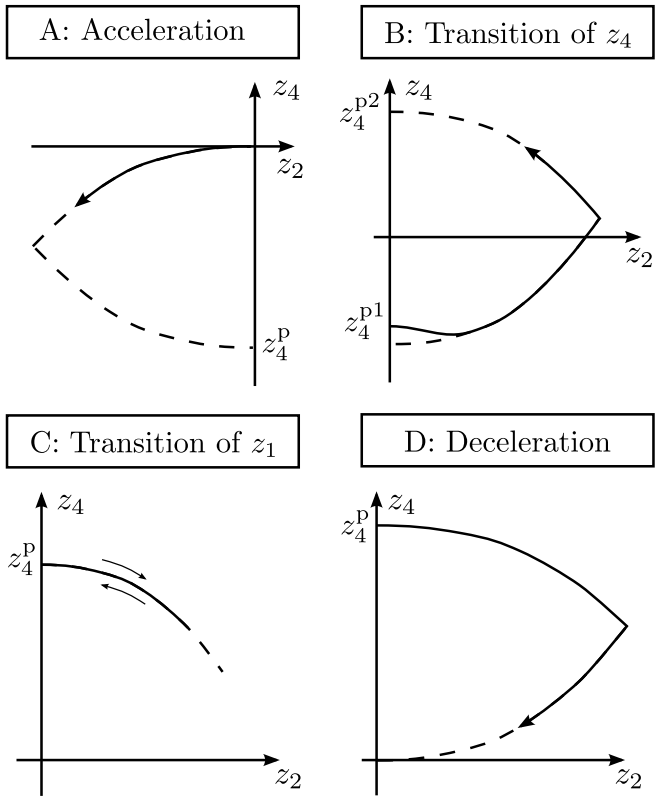

Figure 6. Principle succession of the maneuvers to perform an equilibrium point transition.

Fig. 6 schematically shows the four maneuvers A-D. Between each of them, a waiting phase takes place, in which the second joint circulates at constant rate. The system remains in this parking regime until a configuration is reached which provides the appropriate drift for the next maneuver.

5.4 Simulation Results

To illustrate the equilibrium transition we provide some results of a numerical simulation. In order to keep it simple the start and end values of the joint angles are chosen such that only the necessary maneuvers A and D have to be performed. As parameter value $\eta = 0.9$ is used.

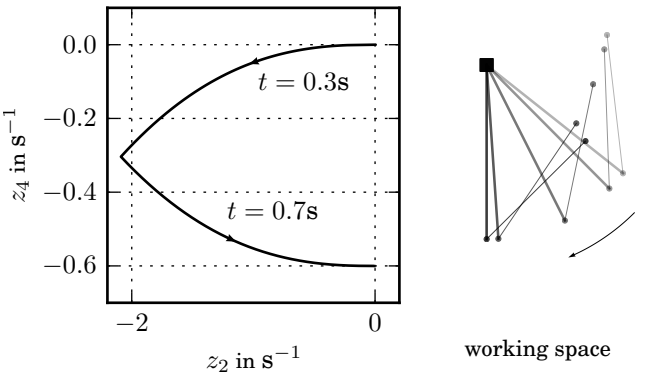

Figure 7. Maneuver A

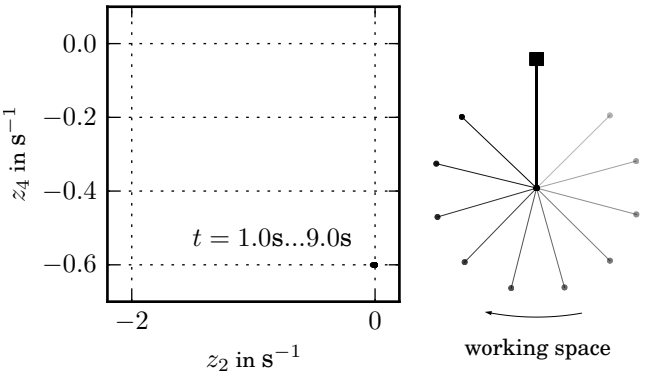

Figure 8. Parking regime

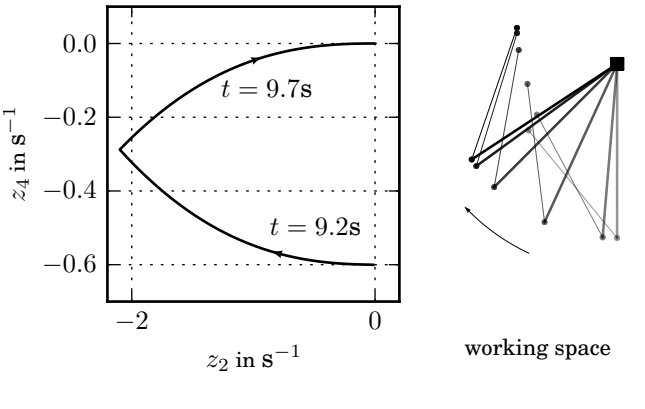

Figure 9. Maneuver D

Figures 7 to 9 show the projection of the system dynamics to the z_2-z_4-plane as well as the manipulator movement in working space. Figure 10 shows the system input v. It becomes obvious that the actuator has only to work

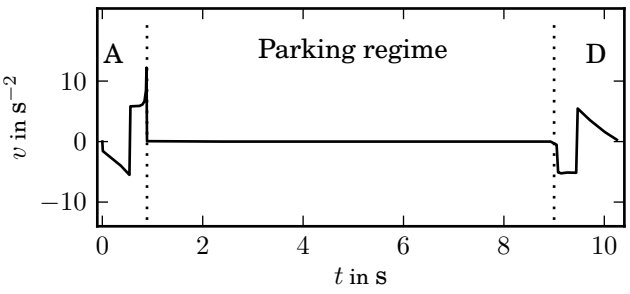

Figure 10. Maneuver D

to increase the system's energy at the beginning and to decrease it at the end. This distinguishes our approach from Suzuki et al. (1996) and De Luca et al. (1997) where modulated periodic inputs are used.

The overall time for equilibrium transition is mainly determined by the length of the waiting phase during the parking regime. The transition time can be influenced by the parameters of the sliding surfaces, more precisely by the absolute value of z_4^{p}, cf. Fig. 6.

6. CONCLUSION AND OUTLOOK

Summarizing, we can state, that with the collection of all four maneuvers nearly all possible equilibrium point transitions can be performed without relying on a holding brake nor on Coulomb friction. Furthermore, the actuator activity is comparatively low since the zero dynamics of the system is exploited.

In the future we want to consider the friction torque in the passive joint explicitly, even if it is small. Furthermore, experimental validation of the control approach is in preparation. First practical results can be found in Knoll and Röbenack (2011).

REFERENCES

Arai, H. and Tachi, S. (1991). Position control system of a two degree of freedom manipulator with a passive joint. *IEEE Transactions on Industrial Electronics*, 30, 15–20.

Ashrafiuon, H. and Erwin, R.S. (2008). Sliding mode control of underactuated multibody systems and its application to shape change control. *International Journal of Control*, 81, 1849–1858.

Bhat, S.P. and Bernstein, D.S. (1998). Continuous finite-time stabilization of the translational and rotational double integrators. *IEEE Transactions on Automatic Control*, 43(5), 678–682.

Brockett, R.W. (1983). Asymptotic stability and feedback stabilization. In R.W. Brockett, R.S. Millmann, and H.J. Sussmann (eds.), *Differential geometric control theory*, 181–191. Birkhäuser, Boston.

Bullo, F. and Lewis, A.D. (2004). *Geometric Control of Mechanical Systems*, volume 49 of *Texts in Applied Mathematics*. Springer-Verlag, New York.

De Luca, A., Mattone, R., and Oriolo, G. (1997). Stabilization of underactuated robots: Theory and experiments for a planar 2R manipulator. In *Proc. of the 1997 IEEE International Conference on Robotics and Automation Albuquerque, New Mexico*, 3274–3280.

Isidori, A. (1995). *Nonlinear Control Systems*. Springer-Verlag, Berlin, 3rd edition.

Knoll, C. and Röbenack, K. (2010). Sliding mode control of an underactuated two-link manipulator. In *Proc. in Applied Mathematics and Mechanics (PAMM)*, 615–616.

Knoll, C. and Röbenack, K. (2011). Konzeption und prototypische Realisierung eines Versuchsstandes zur Regelung eines unteraktuierten Manipulators. In *Tagungsband Mechatronik 2011*, Dresden, Germany, 241–246.

Mahindrakar, A., Rao, S., and Banavar, R.N. (2006). Point-to-point control of a 2R planar horizontal underactuated manipulator. *Mechanism and Machine Theory*, 41(7), 838–844.

Mareczek, J., Buss, M., and Schmidt, G. (1999). Robuste Regelung eines nicht-holonomen, unteraktuierten SCARA-Roboters. *at - Automatisierungstechnik*, 47, 199–208.

Oriolo, G. and Nakamura, Y. (1991). Control of mechanical systems with second-order nonholonomic constraints: Underactuated manipulators. In *Proc. of the 30th IEEE Conf. on Decision and Control*, 2398–2403.

Riachy, S., Orlov, Y., Floquet, T., Santiesteban, R., and Richard, J. (2008). Second-order sliding mode control of underactuated mechanical systems I: Local stabilization with application to an inverted pendulum. *International Journal of Robust and Nonlinear Control*, 18(4-5), 529–543.

Scherm, N. and Heimann, B. (2001). Nichtlineare zeitdiskrete Regelung eines unteraktuierten Manipulators. *at - Automatisierungstechnik*, 49, 107–115.

Slotine, J.J.E. and Li, W. (1991). *Applied Nonlinear Control*. Prentice-Hall, Englewood Cliffs.

Spong, M.W. (1998). Underactuated mechanical systems. In B. Siciliano and K.P. Valavanis (eds.), *Control Problems in Robotics and Automation*, 135–150. Springer-Verlag, Berlin.

Suzuki, T., Koinuma, M., and Nakamura, Y. (1996). Chaos and nonlinear control of a nonholonomic free-joint manipulator. In *Proc. of the 1996 IEEE International Conference on Robotics and Automation*, 2668–2675.

Wichlund, K., Sordalen, O., and Egeland, O. (1995). Control of vehicles with second-order nonholonomic constraints: Underactuated vehicles. In *Proc. of the European Control Conference, Rome, Italy*, 3086–3091.